Technologies for Spacecraft Formation Flying

John Adams, Andrew Robertson, Kurt Zimmerman, Dr. Jonathan How, *Stanford University*

BIOGRAPHY

John Adams is a Ph.D. candidate in the Department of Aeronautics and Astronautics at Stanford University. He received his SB and SM in Aeronautics and Astronautics from MIT. His research involves the use of GPS for autonomous spacecraft navigation.

Andrew Robertson is a Ph.D. candidate in the Department of Aeronautics and Astronautics at Stanford University. He received his SB (1993) from MIT and his MS (1995) from Stanford University. He is researching dynamics and control issues in spacecraft formation flying.

Kurt Zimmerman is a Ph.D. candidate in the Electrical Engineering Department at Stanford University.

Jonathan How is an Assistant Professor in the Department of Aeronautics and Astronautics at Stanford University. He received his B.A.Sc (1987) from the University of Toronto, and his SM (1990) and Ph.D. (1993) from MIT both in the Department of Aeronautics and Astronautics.

ABSTRACT

Differential carrier phase GPS for orbit and attitude determination is emerging as a very promising low cost alternative to more conventional methods, such as horizon sensors, sun sensors, magnetometers, and star trackers. Relative spacecraft position and attitude determination are important for missions involving formation flying, such as those proposed for stellar interferometry under NASA's New Millennium Program, and LEO missions for atmosphere and gravity modeling and for coordinated Earth observing. Our research involves developing a GPS based relative position and attitude sensing system in a laboratory environment for future application on spacecraft formations

Previous research by Zimmerman[1,2] created a fully functional demonstration of spacecraft rendezvous and capture in 2D, in an indoor GPS environment using simulated spacecraft on an air-bearing table. Current work includes extending the previous GPS based sensing to a formation of three prototype spacecraft, and developing the algorithms for formation control. Control of a three-vehicle formation is studied with overhead vision sensing as a surrogate for GPS sensing. Two control architectures, using absolute and relative commands are investigated experimentally.

A layered formation sensing strategy is being investigated, using GPS code phase measurements, code phase with differential corrections, differential carrier phase, and other higher precision measurements in a hierarchy. An analysis of the applicability of a proposed wide area differential GPS correction system to LEO spacecraft navigation, in terms of availability and performance, is presented.

An estimation technique for autonomous integer bias resolution using a motion based technique has been demonstrated in simulation and validated using experimental carrier phase data from a two vehicle formation in the laboratory.

1 INTRODUCTION

Formation flying of multiple spacecraft is an enabling technology for many future space missions, and the Global Positioning System (GPS) will play an important role as a sensor. We define formation flying as the coordinated motion control of a group of vehicles where the vehicle positions relative to each other are important. These vehicles may be groups of trucks, aircraft [3], spacecraft [4], or mobile robots [5]. Results in this paper are presented for spacecraft, but all of these vehicle formation applications share common research problems involving the autonomous sensing and control of groups of vehicles.

The development of formation flying technologies for spacecraft applications will enable the use of a 'virtual spacecraft bus' where multiple distributed spacecraft could be coordinated to act as one. This should enable new scientific missions involving coordinated but distributed measurements, leading to improved stellar interferometry, gravimetry, and synthetic aperture radars. These scientific missions will be made possible because of the increased autonomy, modularity, and robustness provided by the formation flying technologies. These techniques will have the additional benefit of reducing the ground maintenance requirements, thereby significantly lowering the ground operation costs.

Spacecraft formation control will require a measure of the formation states, i.e., the relative attitude and positions of the vehicles. GPS techniques offer some

promising methods to sense these variables, at a much lower cost than conventional spacecraft sensors such as star trackers, horizon and sun sensors, and inertial measurement systems. Our approach is based on the differential carrier phase (DCP) techniques that have already been demonstrated on orbit for attitude determination [10]. DCP GPS can provide high precision (cm level) sensing for relative positioning between spacecraft.

This research has been strongly motivated by two missions currently being planned under the NASA New Millennium Program (NMP) that will require the development of formation flying technologies. They are the New Millennium Interferometer (NMI) and the Earth Orbiter 1 (EO-1) missions (see [6] and [7]). The NMI mission is a formation of three spacecraft in a solar orbit 0.1 AU from the Earth to be used for long baseline optical stellar interferometry. Two of the spacecraft will be light 'collectors', separated by several kilometers, that focus light from a distant star onto an third 'combiner' spacecraft which will form the interference pattern. Note that to form the interference pattern, the optical path between the spacecraft must be controlled to within a fraction of a wavelength of light. To achieve this, a layered control approach is proposed, one layer of which will use DCP GPS sensing using pseudolite transmitters in a *self-constellation* to regulate the formation positions to within a centimeter. This is an example of high **precision** formation flying.

The EO-1 mission is planned to be a co-flight with the Landsat 7 spacecraft. The main scientific goal of the EO-1 mission is to validate the results obtained with the multispectral imager on board Landsat 7 by taking images with a similar instrument on board the EO-1 spacecraft. This objective will be achieved by flying the two spacecraft with the relative distance between them controlled so that both imagers are influenced by the same atmospheric disturbances. In this case, the formation tolerance will be on the order of hundreds of meters, which is an example of **coarse** formation flying. It is also expected that the EO-1 mission will include advances in autonomous orbit determination, using the navigation algorithm developed for the GPS Enhanced Orbit Determination Experiment (GEODE) [8], and the incorporation of a wide area differential GPS correction into this autonomous navigation system.

There are several ongoing research programs at Stanford University into the development and application of GPS technologies to autonomous vehicles [9,10]. Zimmerman [1,2] has demonstrated the use of DCP GPS for spacecraft rendezvous and capture between one active and one passive simulated spacecraft in an indoor laboratory GPS environment. Our current work at Stanford has been focused towards extending Zimmerman's research to the control of a formation of three active vehicles and supporting the NMP mission goals for coarse and precision formation flying. This involves simulation studies of the use of GPS for formation sensing on EO-1, and in particular the use of a wide area differential GPS correction for that mission, and laboratory experiments in the sensing and control of multiple free flying autonomous vehicles. The main areas of research interest fall into the categories of formation sensing and control. In the area of formation control, we are investigating the use of absolute versus relative control architectures, the communication and dataflow requirements generated by the control architecture, and formation trajectory generation. Formation sensing work focuses on improving the autonomy of spacecraft navigation through the use of wide area differential and DCP GPS techniques. In particular, the formation re-initialization problem after loss of GPS lock is being examined.

2 GPS WAAS FOR LEO SPACECRAFT

As part of a layered sensing approach to the formation sensing problem, it is desirable to use a differential GPS technique to determine the absolute position of a spacecraft in the formation to within 1-2m. The GPS Wide Area Augmentation System (WAAS) is an implementation of a differential GPS correction system currently being developed by the FAA that should provide accuracies on that order [11]. For our research into formation flying technologies for NMP EO-1, an analysis was made of the applicability of these WAAS corrections for improving the GPS navigation solution for spacecraft in low earth orbit. The WAAS will use ground stations at known locations to receive GPS satellite signals and calculate corrections for atmospheric errors, and GPS satellite ephemeris/clock errors. The most significant of these errors are introduced by the Selective Availability (SA) corruption. Note that it is anticipated that SA will still be activated during the EO-1 mission time frame. While the atmospheric correction will not be applicable to a LEO spacecraft, the GPS satellite clock and ephemeris correction will be valid.

Before analyzing the performance of an orbit determination method that makes use of the WAAS correction, it is necessary to determine how applicable such a correction will be given a set of potential WAAS ground stations and a spacecraft in LEO. An analysis was done of the visibility of the EO-1 spacecraft and a proposed North American WAAS network of ground stations to the GPS constellation. A computer simulation was created where the motions of the EO-1 satellite, the GPS satellites, and the WAAS reference stations on a rotating earth were calculated. The forces on the spacecraft were modeled as simply a central gravity force

with a spherical earth, and the EO-1 spacecraft was assumed to have omni-directional GPS antenna coverage. The GPS constellation was assumed to be a 24 satellite constellation with the initial ephemeris taken from an update obtained in June, 1995. This set of ephemerides was judged to be representative enough to serve as a general model for the constellation. The EO-1 orbit was assumed to be a polar, circular orbit, with an altitude of 705 km (98.8 min period) and an initial orbit anomaly with a nadir point on the equator. The initial longitude of the EO-1 satellite was varied during the analysis, with a nominal starting longitude of 0 deg.

A set of 15 potential WAAS reference stations was taken from Kee[11]. These reference stations were located entirely in North America and Hawaii, and are representative of a network that would be available during the EO-1 mission time frame.

2.1 Commonly Visible Satellites Results

A series of simulation runs for a single EO-1 orbit were conducted, with varying initial orbit longitude and horizon mask angle for visibility. Figure 2.1 shows the total number of GPS satellites that are visible by both the EO-1 spacecraft and at least one reference station in the WAAS network, over one orbit of EO-1 given an initial orbit longitude of 0 deg. To analyze the effect of the ionosphere, the total number of commonly visible satellites was found for three horizon mask angles. As expected, as the horizon mask angle increases, the number of commonly visible satellites decreases. The minimum number of commonly visible satellites drops from 5 to 3 as the horizon mask angle is increased from 0 to 10 deg. If it is desired at all times during the EO-1 orbit to have a GPS navigation solution using only satellites for which a WAAS differential correction is available, then a minimum of 4 commonly visible satellites is required. This degree of visibility is possible for this orbit with a 5 deg horizon mask angle, which is sufficient to reduce the ionosphere effects on the GPS signals.

To determine if this particular initial orbit longitude was favorable for having commonly visible satellites between EO-1 and the WAAS reference stations, several runs were started at varying initial longitudes. The minimum number of commonly visible satellites over each orbit was found. The simulations indicated that for the 5 deg horizon mask angle, the minimum number of WAAS corrected satellites visible from EO-1 can drop to as low as 2, depending on the initial longitude of the orbit. Thus, using only the North American ground stations, it is possible during the EO-1 orbit that the GPS navigation solution will not be available solely from WAAS corrected satellites.

2.2 Determined vs. Underdetermined Corrections

The previous analysis assumed that a commonly visible satellite need only have view of a single WAAS ground station in the network. Another factor to consider is that to completely solve for the WAAS orbit ephemeris and clock correction for a GPS satellite, the GPS satellite must be in view of at least 4 ground stations. This is the fully 'determined' case, and while a GPS satellite that has view of less than 4 ground stations may be able to get some partial correction information, these satellites are 'underdetermined' in terms of the WAAS correction [11].

The visibility numbers shown in Figure 2.1 were re-analyzed to determine which of the commonly visible GPS satellites are 'determined' or 'underdetermined'. To visualize this data, Figure 2.2 shows two ground tracks of the EO-1 spacecraft, one for an initial orbit longitude of 0 deg and one for 90 deg. The number of determined and underdetermined commonly visible GPS satellites is printed next to the orbit. As expected, the WAAS visibility is best over North America, and is relatively good over much of the northern hemisphere, even at longitudes approaching 180 deg from North America. The visibility is worse in the southern hemisphere and there are times during both orbits where no fully determined WAAS corrected GPS satellites are visible.

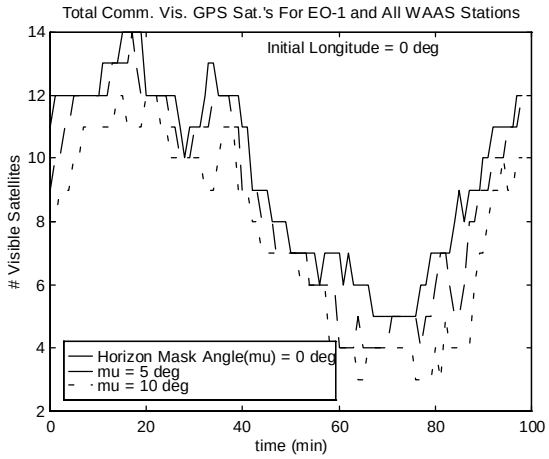

Figure 2.1 - Total commonly visible GPS satellites between EO-1 and the WAAS reference stations over one orbit. Initial EO-1 longitude is 0 deg, and horizon mask angle is varied from 0 deg to 10 deg.

The important point of this graph is that while it previously appeared that for this EO-1 orbit and mask angle a minimum number of four WAAS corrected satellites would be visible for the entire orbit, it can be seen that not all of those visible satellites are fully determined and therefore will not have the full WAAS correction. In fact there is a 4 minute gap from ~60 min to ~64 minutes in the orbit where all the commonly visible GPS satellites are underdetermined for the WAAS correction.

2.3 Implications for Autonomous Navigation

Some interesting conclusions can be drawn from this analysis. First, the common visibility between the EO-1 spacecraft and the WAAS stations is surprisingly good, but this makes sense given the high orbits of the GPS satellites. It should also be noted that for many cases, these satellites are being viewed close to the horizon which will degrade their signals. While these satellites might not be selected to compute the navigation solution without WAAS, the availability of the WAAS correction will strongly influence this selection process.

The next step to add to this analysis would be to add an error model for the WAAS corrected satellites that would take into account their viewing geometry and whether or not they are fully determined or underdetermined. In this way, the navigation solution for the EO-1 spacecraft could be calculated at each point, and it could be determined where it does and does not make sense to use the WAAS correction in the orbit. The implication of this is that the WAAS visibility and error model must be an integral part of the overall orbit determination scheme. The interaction between the WAAS model and the orbit determination algorithms (such as GEODE [8]) must be analyzed to see the effect of using WAAS for orbit determination.

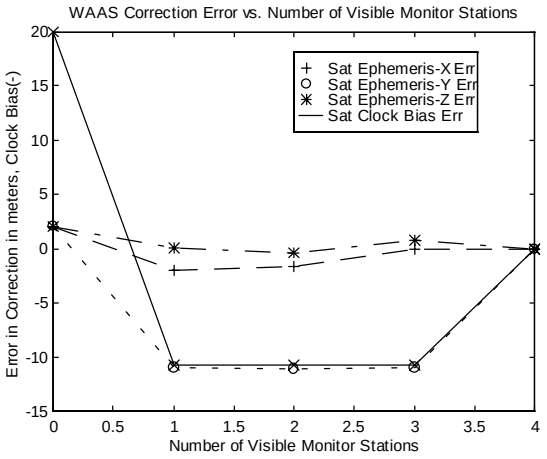

Figure 2.3 - WAAS Correction Error vs. Number of Visible Monitor Stations for Underdetermined Case.

Figure 2.3 shows the error in the WAAS correction message for underdetermined GPS satellites. This error is highly dependent on the viewing geometry to the visible monitor stations, but gives an idea of the degradation of the WAAS correction when fewer than 4 monitor stations are visible.

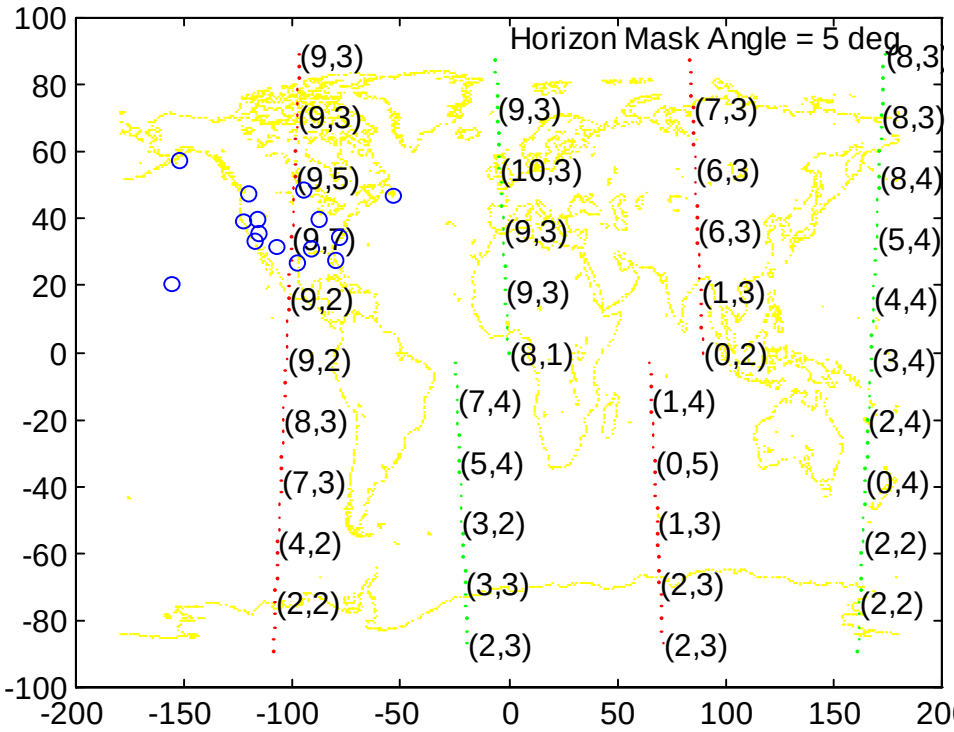

Figure 2.2 - EO-1 ground track for 2 orbits; initial longitude = 0deg and90 deg. Number of fully determined and underdetermined commonly visible satellites between EO-1 and the WAAS reference stations are shown along the ground tracks, (#determined, #underdetermined). WAAS reference station locations plotted with circles.

3 FORMATION FLYING LABORATORY

To study formation flying issues related to the precision NMI mission, a formation flying testbed has been created in the Stanford Aerospace Robotics Laboratory. It consists of 3 active free-flying vehicles, and one passive target vehicle, moving on a 12'X9' granite table top (see Figure 3.1). These air cushion vehicles simulate the zero-g dynamics of a spacecraft formation in a plane. The vehicles are propelled by compressed air thrusters, and two of the three are also equipped with momentum wheels and rate gyros for controlling their rotation. Each vehicle has onboard computing and batteries, and communicates with the other vehicles via a wireless ethernet, making them self-contained and autonomous.

Figure 3.1 - Formation Flying Testbed

In the previous experiments by Zimmerman[1,2], a complete indoor GPS environment was constructed. This consists of six ceiling mounted pseudolite transmitters broadcasting the L1 carrier phase signal modulated by a unique C/A code, with no navigation data. One transmitter is designated the 'master pseudolite' and transmits a 50 bps data message modulated on top of the C/A code, which contains timing information for synchronizing the carrier phase measurements of multiple receivers in the laboratory to within one millisecond epoch. It is this synchronization that enables differential carrier phase measurements to be made between receivers on separate vehicles. Each vehicle has a six channel Trimble TANS Quadrex receiver with customized software. Currently, the carrier phase information from each vehicle is collected by a single master vehicle, at a 10 Hz rate, and used to solve for the relative positions and attitudes of the vehicles in the formation.

Additions that have been made to the experiment set up by Zimmerman include the addition of two more actively controlled vehicles to replace a passive target vehicle, and equipping all three vehicles with GPS receivers and antennas.

There is an overhead vision system mounted above the table, and each object on the table is tagged with a unique LED pattern that can be tracked. The vision system has an absolute accuracy of 1 cm throughout the workspace, and a measurement repeatability on the order of less than a millimeter. It is useful for validation of the position solutions generated by GPS sensing.

Experimenting with spacecraft formation flying in a laboratory environment presents several challenges. There are problems involved with getting multiple vehicles to move in a coordinated manner in a limited workspace and problems in getting an indoor laboratory GPS sensing system to work. To create this indoor GPS environment, Zimmerman had to deal with issues that are very different from GPS sensing using the NAVSTAR satellites. Some of the main differences are:

- Large near/far signal power variations
- Non-planar carrier wavefronts
- High multipath environment
- Receiver/transmitter synchronization
- No pseudorange information is used

4 SPACECRAFT AUTONOMOUS FORMATION CONTROL

The NMI mission will require three vehicles to maintain a formation while observing a celestial target. When a new target is desired, the vehicles will have to maneuver to collect light from the new target. It may be desirable to maintain formation during this maneuver. An experiment was performed with the formation flying testbed on this premise; that three vehicles perform a maneuver while maintaining formation.

4.1 Formation Control Architectures

The formation considered here is a line formation. The vehicles start staggered 0.5m apart along the y direction. The maneuvers are simple displacements of the line formation in x - 1m forward, then 1m back. During maneuvers, the control architecture should maintain the 0.5m separations between vehicles as well as move the vehicles equally in x.

Two architectures for multi-vehicle control were considered: absolute and relative control. The absolute control architecture has a central controller that sends position and velocity commands to each vehicle. Each vehicle tries to regulate its own absolute position to the commanded value. The relative control architecture

sends absolute position/velocity commands to only one vehicle (the "leader"). Each of the other vehicles (the "followers") tries to regulate its own position to maintain the line formation (i.e. they follow the leader).

Absolute control offers potential advantages in performance during maneuvers because the central controller sends the desired trajectory to each vehicle simultaneously, so they will start moving at the same time. In contrast, each follower vehicle under relative control only starts moving when it senses the relative position between itself and the leader changing (i.e., the leader has already started moving). For instance, in the NMI case, one vehicle - the collector - may have relative sensors (e.g. GPS-like transceivers) plus absolute sensors (such as star trackers) and the other vehicles may have only relative sensors. When a maneuver is needed, the collector may travel to point at the new target and the other vehicles will have to keep up, feeding back only on the sensed movement of the collector.

4.2 Experiment

The three active free-flying vehicles were arranged in a line formation. The formation was commanded to maneuver one meter forward and then one meter back. Position and orientation data was taken (from the overhead vision system) for two minutes with each maneuver lasting thirty seconds. This experiment was performed for both absolute and relative control. The only factor varied between runs was how position and velocity commands were generated on the "follower" vehicles. The vehicles attempted to move to commanded positions using available actuators. Thruster control allowed a deadband of ≈ 3 cm in position for two of the vehicles and ≈ 7 cm in position for the third.

Figures 4.2 and 4.3 show the time histories for the three vehicles' x-position on the table for each control architecture. The vehicles were commanded to move in the x direction, while the formation was arranged in a line along the y direction (see figure 4.1).

The performance measure **p** in this case is the norm of the relative position error vehicle to vehicle.

$$p = \sqrt{(\Delta X_{robot1-2})^2 + (\Delta X_{2-3})^2 + (\Delta X_{3-1})^2}$$

The goal is to maintain formation during a maneuver, thus vehicle relative positions should remain constant (at some commanded value) throughout the maneuver. The sensor used in this experiment was the laboratory overhead vision system. The vision system acts as a surrogate for GPS sensing in this case. Future experiments will include GPS as a sensor, but the focus here is on comparing formation control architecture performance during the maneuver. Figure 4.4 compares the performance of the two architectures during the first maneuver.

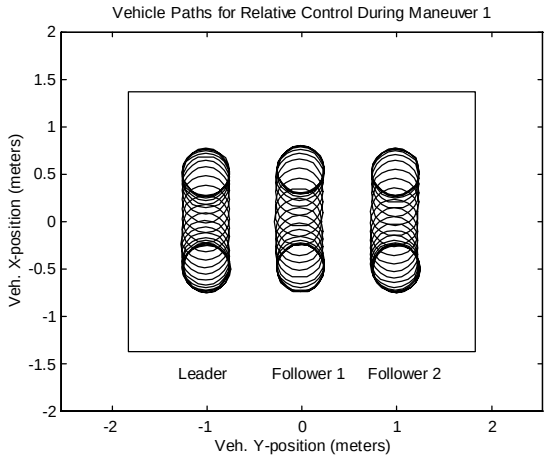

Figure 4.1 - Vehicle positions during maneuver. Granite table shown in outline.

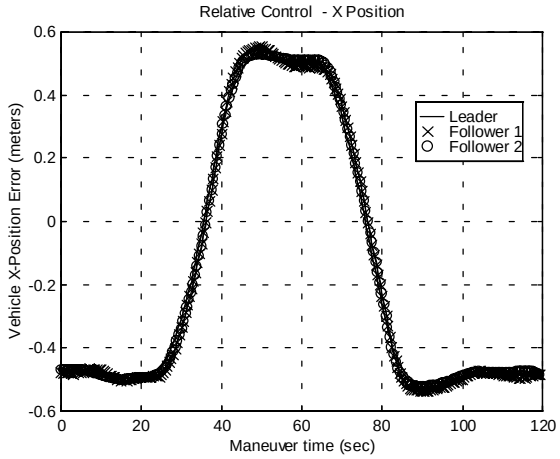

Figure 4.2 - Vehicle position (X) history for relative control.

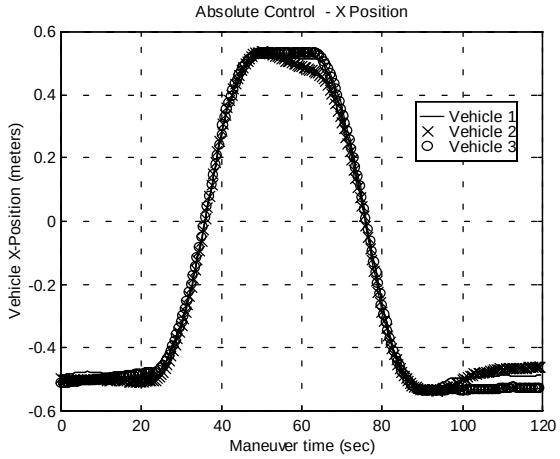

Figure 4.3 - Vehicle position (X) history for absolute control.

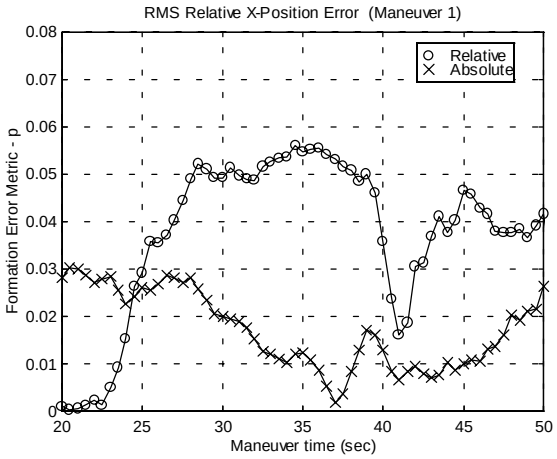

Figure 4.4 - Formation error magnitude 'p' during maneuver.

4.3 Results

In the static case (no maneuvers), relative control allows better performance because the follower vehicles feed back what is important, the relative positions. This is apparent in the initial conditions in figure 4.4, which reflect 20 seconds of control with no maneuver commanded. During the maneuver, absolute control works better because the central controller tells all three vehicles about the maneuver at the same time. There is lag in the follower vehicles' motions under relative control because the leader must start moving before the follower vehicles can sense that a maneuver is needed. This can be seen in figure 4.4.

It is clear that both architectures are effective for formation control. A combined approach would perform even better, but would be more costly in terms of computation power and communication bandwidth, so further investigations are required. There are clearly other control issues to be investigated as well. For instance, a decentralized control architecture (with no inter-vehicle communication) could be compared to a centralized control architecture (with all actuator commands determined by a central controller based on sensor information from all vehicles). This formation flying testbed enables investigation of these control issues, and will allow experimental validation of the control techniques using GPS sensors.

5 FORMATION INITIALIZATION PROBLEM

5.1 Integer Ambiguity Bias Estimation

To achieve formation sensing and control to the centimeter accuracies necessary for a mission such as the New Millennium Interferometer, a hierarchical sensing approach must be taken, with sensors with less accuracy aiding the initialization of more precise ones. For example, if a spacecraft formation is in LEO, a position solution for the vehicles in the formation might first be determined to within 100m using code phase GPS, to within 1-2m using a differential GPS correction, then to within centimeters using DCP GPS techniques, and finally to within the tolerances necessary for interferometry using optical sensors.

The problem examined in this section is the one of re-establishing DCP formation sensing once carrier phase lock has been lost. This will be required to happen routinely as satellites either come into view or are lost from view, and will also be necessary for cases of cycle slip or the rare event of a satellite failure.

Vehicle state and the integer wavelength ambiguity biases associated with carrier phase measurements can be estimated from phase differences. For the attitude determination problem (Cohen[12]), where there is no relative antenna motion and phase measurements are made on the same receiver, the integer biases can be estimated using only single differences of phase measurements. For the flexible structure problem, there is relative motion of the antennas, but the phase differences are still made from the same receiver, so only single differences are necessary for the bias estimation. For the autonomous helicopter control experiment, (Conway[13]), separate vehicles and separate receivers are used to generate the carrier phase differences. But since their experiment uses carrier phase measurements from the NAVSTAR constellation rather than a pseudolite constellation with much less accurate clocks, there is no transmitter clock bias to eliminate, single difference carrier phase measurements can be used.

However for our experiment, it is necessary to use carrier phase double differences to account for the time biases in the pseudolite transmitters as well as the receivers. Once the carrier phase is locked onto for a given satellite, the initial phase integer ambiguity bias can be estimated along with the state using a batch nonlinear least squares estimation algorithm.

The measurement equation for the carrier phase double difference for master antennas j, between vehicles i1 and i2, and between transmitters k1 and k2, is;

$$\nabla\Delta\phi_{(i1-i2)j(k1-k2)} = \left|\underline{D}_{i1jk1}\right| - \left|\underline{D}_{i2jk1}\right| - \left|\underline{D}_{i1jk2}\right| + \left|\underline{D}_{i2jk2}\right| - b_{(i1-i2)j(k1-k2)}$$

'D' is the distance vector from transmitter k to the antenna j on vehicle i, and 'b' is the initial bias due to the differences in integer wavelength ambiguity for each antenna.

The number of measurements is the number of independent vehicle pairs times the number of transmitters minus one ($N_M = N_P*(N_T - 1)$). For our

laboratory setup with 3 vehicles and 6 transmitters, this gives 10 independent double difference measurements. The nonlinear measurement equation is;

$$\underline{z} = \nabla\Delta\underline{\phi} = \underline{d}(\underline{F}) + \underline{b} = \underline{h}(\underline{F}, \underline{b}) = \underline{h}(\underline{Y})$$

where, $\underline{F} = \left[\underline{x}_1^{\,T} \quad \underline{x}_2^{\,T} \quad \cdots \quad \underline{x}_n^{\,T}\right]^T$ = formation state

and, $\underline{Y} = \left[\underline{F}^T \;\vdots\; \underline{b}^T\right]^T$ = formation state plus bias states

$\underline{d}$ = function of distance from vehicles to transmitters

$\underline{b}$ = initial integer ambiguity biases for each measurement

$\underline{x}_n$ = position of vehicle # n

n = total number of vehicles in formation

The number of states is equal to the number of vehicles in the formation times the number of states per vehicle plus the number of bias states. There is one bias state per measurement, so for our laboratory setup with 3 vehicles, 3 states per vehicle, and 10 measurements, there are 19 states.

The nonlinear measurement equation, h(Y), can be linearized about the nominal states (denoted by the bar over the variable);

$$\frac{d\underline{z}}{d\underline{Y}} = H(\overline{\underline{Y}}) \approx \frac{\delta\underline{z}}{\delta\underline{Y}} \quad , \quad \delta\underline{z} = \left[H(\overline{\underline{F}}) \vdots I\right]\delta\underline{Y}$$

The object is determine an optimal estimate of the states, Y, given the measurements, z. But since the number of states is greater than the number of measurements for any given measurement epoch, the problem is underdetermined. To solve for the bias states, measurements must be collected over k measurement epochs and stacked to form a non-linear batch least squares problem of the form;

$$\begin{Bmatrix} \delta\underline{z}^1 \\ \delta\underline{z}^2 \\ \vdots \\ \delta\underline{z}^k \end{Bmatrix} = \left[\begin{array}{cccc:c} H(\overline{\underline{F}}^1) & 0 & \cdots & 0 & I \\ 0 & H(\overline{\underline{F}}^2) & \cdots & 0 & I \\ \vdots & \vdots & \ddots & 0 & \vdots \\ 0 & 0 & 0 & H(\overline{\underline{F}}^k) & I \end{array}\right] \begin{Bmatrix} \delta\overline{\underline{F}}^1 \\ \delta\overline{\underline{F}}^2 \\ \vdots \\ \delta\overline{\underline{F}}^k \\ \delta\overline{\underline{b}} \end{Bmatrix}$$

$$\delta\underline{z}_T = H_T(\overline{\underline{Y}})\delta\underline{Y}_T$$

$$\delta\underline{z}_T = \underline{z}_T - \overline{\underline{z}}_T = H_T(\overline{\underline{F}})(\hat{\underline{Y}}_T - \overline{\underline{Y}}_T)$$

$$\hat{\underline{Y}}_T = \overline{\underline{Y}}_T + \left(P_0 + H_T^T R^{-1} H_T\right)^{-1} H_T^T R^{-1}(\underline{z}_T - \underline{h}_T(\overline{\underline{Y}}_T))$$

At each measurement update, the last equation is iterated upon until the estimated states converge. As proposed by Cohen [13] for the attitude determination problem, motion of the vehicle, or motion of the transmitters, or both, will provide enough geometry change that the collected measurements will be independent and the linearized measurement matrix H_T will be full column rank. For the formation problem, it is necessary to design vehicle maneuvers that ensure the observability of the integer bias states while minimizing the costs associated with fuel expenditure, time, and disruption of the overall formation geometry.

5.2 Simulation of Integer Bias Estimation Problem

The bias estimation problem was solved in simulation for a variety of vehicle maneuvers, assuming a level of noise on the state estimate during re-acquisition of the integer biases that would be close to the accuracy expected of GPS code phase position fixed augmented by a WAAS correction (i.e. standard deviation of ≈ 1 m). The standard deviation of the double difference phase measurement was conservatively modeled to be 5 cm, which is approximately twice what is seen in our laboratory measurements in a high multipath environment. Table 5.1 compares the different trajectories by the minimum singular value of the $(H_T^T H_T)$ matrix, which is a measure of the inverse covariance of the state estimate. Increasing the minimum singular value of $(H_T^T H_T)$ reduces the largest potential state error covariance. The table also shows the relative merits of the different initialization trajectories in terms of fuel, time, and formation disturbance costs. To minimize the formation disturbance, initialization trajectories that do not involve relative motion between the vehicles are favored. To minimize the fuel requirements for an initialization maneuver, straight line constant velocity trajectories are best. But straight line trajectories do not always provide the geometry change necessary to make the estimation problem observable in the minimum amount of time, as a circular or spinning formation trajectory would.

Figure 5.2.1 shows a plot of the circular formation trajectory, which was found to have the best geometry change for the bias estimation problem, and Figure 5.2.2 shows that the bias estimate errors converge to close to zero in less than 5 iterations of the nonlinear batch least squares routine. Figure 5.2.3 shows a plot of the norm of these bias errors and that this error is converging.

While this estimation algorithm works for this initialization trajectory in our laboratory setup, it only works because the close range of the transmitters provides a large geometry change for the motion of the vehicles. For the same trajectory, if the transmitters are moved farther away, the estimation problem becomes more poorly conditioned.

Trajectory Type	Min. SVD ($H_T^T H_T$)	Fuel Cost	Time Cost	Lost Formation Cost
Circular	6.1×10^{-6}	High	High	Med
Straight Line	1.3×10^{-6}	Low	Low	Low
Relative Motion	$.67 \times 10^{-6}$	Med	High	High
L-shaped	$.5 \times 10^{-6}$	Med	Med	Med
Non-planar	$.01 \times 10^{-6}$	Low	Low	Low

Table 5.1 - Comparison of Initialization Trajectories

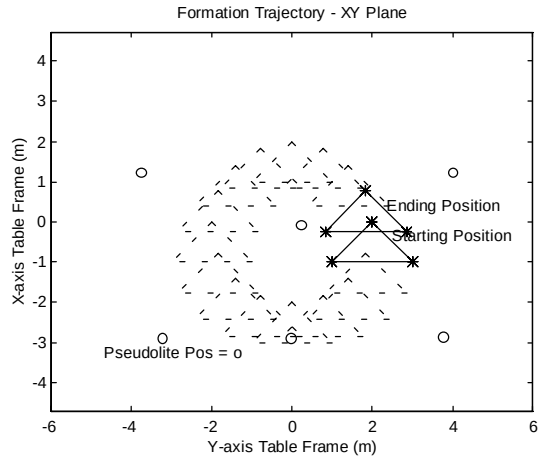

Figure 5.2.1 - Circular Initialization Trajectory

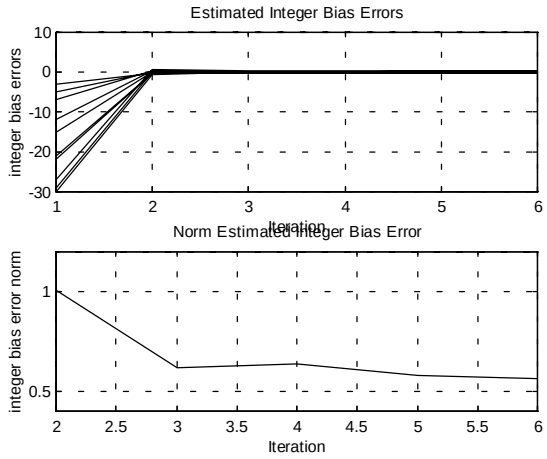

Figure 5.2.2 and 5.2.3 - Error and norm of the error in estimated integer biases over batch least squares iteration.

To alleviate this problem, we have suggested the use of on-board pseudolite transmitters on the vehicles in the formation to supplement the double difference phase measurements. In a deep space mission, such as the New Millennium Interferometer, these would be the only transmitters available. For this case, the minimum number of vehicles that must be in the formation to provide the necessary double difference phase measurements is;

(# vehicles -1)*(# transmitters -3) > # formation states

For the self-constellation case, where each vehicle in the formation carries a transmitter, this results in a minimum constellation size of seven vehicles to employ the same double difference technique used in the laboratory. This would change if the transmitter and receiver on a given vehicle were slaved to the same clock. This eliminates the separate receiver and transmitter clock biases and allows the use of single difference phase measurements between separate vehicles.

5.3 Experimental Validation of Integer Bias Estimation Algorithm

The nonlinear batch least squares bias estimation algorithm was validated using experimentally collected double difference phase measurements from the formation flying testbed vehicles. The experimental data was collected on a formation of 2 vehicles that were connected together with a rigid support (see Figure 5.3.1). The formation was moved through a variety of maneuvers, and vehicle position and double difference carrier phase measurements between the master antennas on the two vehicles were recorded. Arbitrary biases were then added to the phase difference data and then estimated using the batch least squares routine. The plot in Figure 5.3.2 shows the position of the vehicles for a typical spinning initialization maneuver and Figure 5.3.3 shows that the bias estimates do converge on the correct values for this experimental data, as was predicted by the bias estimation simulations.

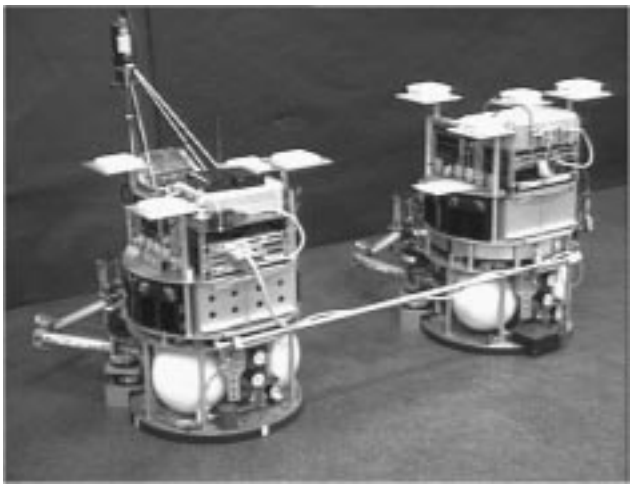

Figure 5.3.1 - Fixed 2 vehicle configuration for experimental bias estimation validation runs.

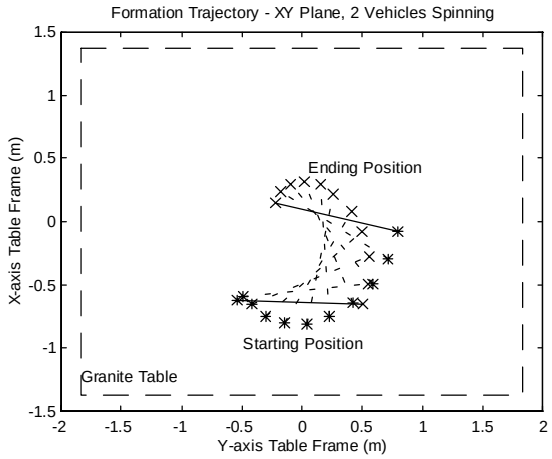

Figure 5.3.2 - Formation trajectory (spinning) for 2 vehicle configuration for experimental bias estimation validation run.

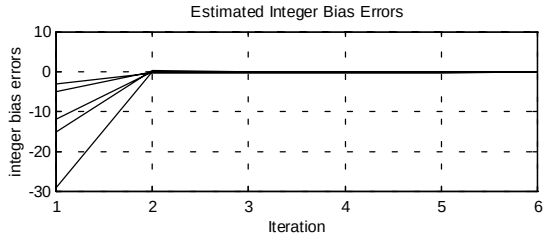

Figure 5.3.3 - Integer bias estimation errors for experimental validation run.

6 CONCLUSIONS

This paper has presented a summary of our ongoing research efforts into the control of formation flying spacecraft, and the use of GPS technologies for spacecraft formation sensing. A formation flying testbed has been constructed in the laboratory using air-cushion vehicles on a granite table, with both GPS and an overhead vision system as sensors. Indoor pseudolite transmitters generate the GPS signals. An analysis of the applicability of using a GPS WAAS correction for LEO spacecraft navigation is presented, along with experimental validations of two formation control architectures. A nonlinear batch least squares estimation algorithm is presented for the solution of the formation integer bias initialization problem, along with a validation test using experimentally collected carrier phase data.

ACKNOWLEDGMENTS

This research is supported under NASA contract 960331, with contract monitor Guy Man of the Jet Propulsion Laboratory. The authors would like to thank Frank Bauer of NASA Goddard Space Flight Center for his support. They would also like to acknowledge the help of Harris Teague in the formulation of the integer estimation problem, and Trimble Navigation, Inc., for their permission to modify the Trimble TANS software for use in this research.

REFERENCES

[1] Zimmerman, K., "Differential Carrier Phase GPS Techniques for Space Vehicle Rendezvous", Proceedings of the Institute of Navigation GPS-94 Conf., Sept. 20-23, 1994, Salt Lake City, UT, vol.2, pg. 1693.

[2] Zimmerman, K., "Experimental Demonstration of GPS for Rendezvous Between Two Prototype Space Vehicles", Proc. of the Institute of Navigation GPS-95 Conf., Sept. 12-15, 1995, Palm Springs, CA, vol. 2, pg. 1905.

[3] Speyer, J.L., Wolfe, J.D., Chichka, D.F., "Decentralized Controllers for Unmanned Aerial Vehicle Formation Flight", AIAA Guidance Navigation and Control Conf, San Diego, CA, July 29-31, 1996, AIAA 96-3833.

[4] Vassar, R.H., Sherwood, R.B., "Formationkeeping for a Pair of Satellites in a Circular Orbit", AIAA Guidance, vol. 8, no. 2, March-April 1985, pg. 235.

[5] Desai, J., Wang, C., Zefran, M., Kumar,V., "Motion Planning for Multiple Mobile Manipulators", Proceedings of the 1996 IEEE Int'l Conf. on Robotics and Automation, Minneapolis, MN, April, 1996, pg. 2073.

[6] Lau, K., Lichten, S., Young, L., "An Innovative Deep Space Application of GPS Technology for Formation Flying Spacecraft", AIAA Guidance Navigation and Control Conf., San Diego, CA, July 29-31, 1996, AIAA 96-3819.

[7] Guinn, J.R., Boain, R.J., "Spacecraft Autonomous Navigation for Formation Flying Earth Orbiters Using GPS", AIAA/AAS Astrodynamics Specialists Conference, San Diego, CA, July 29-31, 1996, AIAA 96-3655.

[8] Bauer, F., Lightsey, E.G., Leake, S., McCullough, J., O'Donnell, J., Hartman, K., Hart, R., "The GPS Attitude Determination Flyer (GADFLY): A Space-Qualified GPS Attitude Receiver on the SSTI-Lewis Spacecraft", Proceedings of the Institute of Navigation GPS-95 Conference, Sept. 12-15, 1995, Palm Springs, CA, vol. 1, pg.555.

[9] O'Connor,M., Elkaim,G., "Kinematic GPS for Closed-Loop Control of Farm and Construction Vehicles", Proc. of the Institute of Navigation GPS-95 Conf., Sept. 12-15, 1995, Palm Springs, CA, vol. 2, pg. 1261.

[10] Lightsey,E. G., Cohen,C. E., "Development of a GPS Receiver for Reliable Real-Time Attitude Determination in Space", Proc. of the Institute of Navigation GPS-94 Conf., Sept. 20-23, 1994, Salt Lake City, UT, vol.2, pg. 1677.

[11] Kee, C., "Wide Area Differential GPS," Global Positioning System: Theory and Applications, Vol. II, ed. B.W. Parkinson and J.J. Spilker, Jr., AIAA, 1996.

[12] Cohen, C. E., "Attitude Determination Using GPS", Ph.D. Thesis, Stanford University, Dept. of Aeronautical and Astronautical Engineering, December 1992.

[13] Conway, A. R., "Autonomous Control of an Unstable Model Helicopter Using Carrier Phase GPS Only", Ph.D. Thesis, Stanford University, Dept. of Electrical Engineering, March 1995.

Filename:	IONPAPER.DOC
Directory:	C:\GPS\RESEARCH\IONSTUFF
Template:	C:\WORD\TEMPLATE\NORMAL.DOT
Title:	Technologies for Spacecraft Formation Flying
Subject:	
Author:	John Carl Adams
Keywords:	
Comments:	
Creation Date:	08/23/96 9:43 PM
Revision Number:	234
Last Saved On:	09/18/96 10:14 AM
Last Saved By:	John Carl Adams
Total Editing Time:	1,539 Minutes
Last Printed On:	07/23/97 12:12 PM

As of Last Complete Printing

Number of Pages:	10
Number of Words:	5,678 (approx.)
Number of Characters:	32,370 (approx.)